Semiconductive, One-Dimensional, Self-Assembled Nanostructures Based on Oligopeptides with π-Conjugated Segments

ARTICLE *in* CHEMISTRY - A EUROPEAN JOURNAL · MARCH 2011

Impact Factor: 5.73 · DOI: 10.1002/chem.201003760 · Source: PubMed

9 AUTHORS, INCLUDING:

Yinghui Sun
Soochow University (PRC)
33 PUBLICATIONS **1,193** CITATIONS
SEE PROFILE

Lin Jiang
Soochow University (PRC)
50 PUBLICATIONS **1,403** CITATIONS
SEE PROFILE

Wencke Adriaens
Technische Universiteit Eindhoven
8 PUBLICATIONS **318** CITATIONS
SEE PROFILE

CHEMISTRY
A EUROPEAN JOURNAL

DOI: 10.1002/chem.201003760

Semiconductive, One-Dimensional, Self-Assembled Nanostructures Based on Oligopeptides with π-Conjugated Segments

Yinghui Sun,[a] Lin Jiang,[a] Klaus C. Schuermann,[b] Wencke Adriaens,[c] Li Zhang,[a] Freddy Yin Chiang Boey,[a] Luisa De Cola,[b] Luc Brunsveld,[c] and Xiaodong Chen*[a]

One-dimensional (1D) micro- and nanostructures based on the programmed self-assembly of π-conjugated molecules are of increasing interest for the rapid development of organic and supramolecular electronics.[1,2] Biomolecules, such as DNA and peptides, have significant applications as building blocks for constructing programmed micro- and nanostructures.[3–6] Molecules based on oligopeptides can similarly assemble into 1D nanostructures, which could contribute to fields, such as tissue engineering, reparative and regenerative medicine, and drug delivery.[5,7] 1D nanostructures based on molecules of oligopeptides and π-conjugated components feature electronic and possibly optoelectronic properties, which are critical for the development of functional supramolecular nanodevices. It has been demonstrated that π-conjugated organic components (e.g., oligothiophene,[8,9] naphthalene,[10] and perylene)[11,12] linked to oligopeptides can form 1D structures, but the π-electron-functionalized groups were typically embedded within the oligopeptide motifs (i.e., nonconductive components), making it difficult to fabricate nanoelectronic devices and characterize the conductivity directly.[8–14] Herein we demonstrate how terminally functionalized π-conjugated peptides assemble into 1D nanostructures to give strong π–π intermolecular electronic communication, which is confirmed by direct-conductivity measurements for the first time.

A new molecule (**1**, Figure 1A) with an oligopeptide (LLKK) and a π-conjugated segment (anthracene) was designed and synthesized (see experimental section). The peptide building block, LLKK, was selected because of its well-known β-sheet-forming characteristics.[9] This property of the peptide segment was envisioned to constitute the main driving force for the formation of 1D nanostructures and the key factor in controlling the preferential growth in one direction.[15] Anthracene was chosen as the π-electron functional group because of its demonstrated tendency to form anisotropic structures through π–π stacking during the self-assembly process.[16,17] Therefore, the specific combination of the β-sheet-forming peptide element and the π–π stacking anthracene was expected to assemble **1** into 1D, conductive, supramolecular nanostructures.

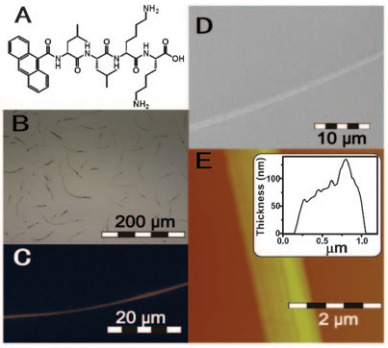

Figure 1. A) Molecular structure of **1**, B) optical microscopy image of self-assembled fibres, C) fluorescence emission image of the ribbon structure excited through a 370–390 nm band-pass filter, D) SEM, and E) AFM images of the fibrous nanostructures on silicon substrate as well as the height profile of the fibrous structure (inset).

The supramolecular assemblies were prepared through a casting assembly method[18] that brings a saturated benzene solution of **1** onto silicon substrates at room temperature. Characterization of the assemblies by using various microscopy techniques clearly showed the formation of 1D fibre-like nanostructures (Figure 1B–E). AFM, optical microscopy, and SEM measurements revealed formation of flexible, 1D, fibrous nanostructures with lengths ranging from 60 to 100 μm and typical heights and widths of 40–120 nm and 1.0±0.1 μm, respectively (Figure 1E). There are two key factors to the self-assembly in the organic solvent: 1) the hydrophilic parts of peptides form β sheets through hydrogen-bonding interactions inside of the ribbon structures,[9] and 2) the hydrophobic parts of the anthracene units form π–π-stacking at the edge of these ribbon microstructures.[18,19]

[a] Dr. Y. Sun,[+] Dr. L. Jiang,[+] Dr. L. Zhang, Prof. F. Y. C. Boey, Prof. X. Chen
School of Materials Science and Engineering
Nanyang Technological University
50 Nanyang Avenue, 639798 (Singapore)
Fax: (+65) 67911604
E-mail: chenxd@ntu.edu.sg

[b] Dr. K. C. Schuermann, Prof. L. De Cola
Physikalisches Institut and Center for Nanotechnology (CeNTech)
Westfälische Wilhelms-Universität Münster
Münster, 48149 (Germany)

[c] W. Adriaens, Prof. L. Brunsveld
Laboratory of Chemical Biology
Department of Biomedical Engineering
Technological University Eindhoven
Eindhoven (The Netherlands)

[+] Y. Sun and L. Jiang contributed equally to this work.

Supporting information for this article is available on the WWW under http://dx.doi.org/10.1002/chem.201003760.

Absorption and fluorescence spectroscopy confirmed the strong π–π stacking of the anthracenes within the 1D nanostructures. A solution of **1** in water shows absorption bands at 331, 346, 363, and 383 nm, typical of the anthracene moiety (Figure S2 in the Supporting Information). Also, compound **1** in water has a strong photoluminescence with the most intense emission maximum at 414 nm (Figure 2A),

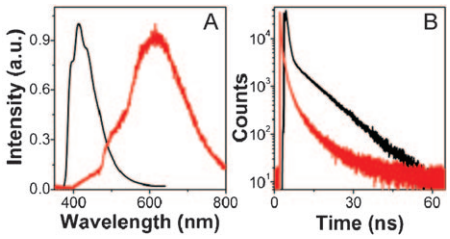

Figure 2. A) Emission spectra and B) fluorescence-lifetime-decay traces of **1** in an aqueous solution (black) and as 1D, self-assembled structures (red, the assembled structures were measured as solid with a confocal microscope).

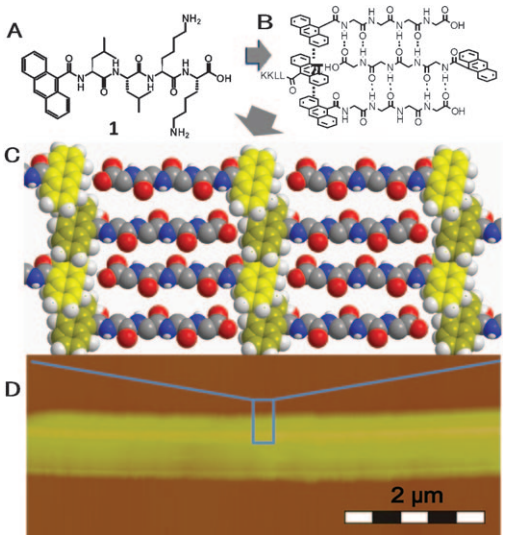

Figure 3. A) Molecular structure of **1**, B) energy-minimized β sheets and π–π stacks, C) schematic diagram of the intermolecular arrangement, and D) an AFM image of the nanofibres on a silicon wafer.

which represents a typical emission from anthracene monomers.[20] However, the solid, 1D, fibrous nanostructures formed by **1** showed an emission spectrum without structure and a broad maximum at 616 nm (notable redshifted by 200 nm compared with **1** in water) as observed by fluorescence spectroscopy (Figure 2A) and fluorescence microscopy measurements (Figure 1C). The redshifted emission of the 1D nanostructures can be attributed to the strong intermolecular π–π stacking of the anthrancenes within the 1D nanostructures.[18,21] Additionally, the redshift suggests stacking of two neighboring anthracene units in a head-to-tail arrangement (or J-aggregate),[22] typically leading to strong coupling between the anthracene-monomer transition dipoles. Fluorescence-lifetime measurements showed that the average lifetime of **1** in the ribbon structures is 0.71 ns, significantly shorter than the lifetime of **1** in aqueous solution (4.64 ns, Figure 2B). This lifetime decrease further proofs the formation of J-aggregates by the anthracene units.[22,23] In addition, the quantum yield of compound **1** (solid state) is 0.08, which is smaller than that of 9-anthracenecarboxylic acid (0.13) that cannot form ordered structures. This further suggests that the intermolecular hydrogen bonding in the peptide β sheets helps to enhance the π–π interaction between anthracenes, and therefore decreases the quantum yield. The observed strong π–π couplings of the anthracene units within the 1D nanostructures indicate efficient π–π electronic communication. This is an important requirement for the formation of nanoelectronic devices based on 1D nanostructures of π-conjugated molecules. From these experimental data, we proposed the model of a 1D nanofibre structure of **1**, as shown in Figure 3. The working model (Figure 3B and C) shows the most probable formation of antiparallel β sheets and π–π stacking that yield layered 1D structures (side-substituted groups were omitted for clarity). The existence of antiparallel β sheets facilitates the formation of π–π stacking between the adjacent anthracene groups at alternating ends of each oligopeptide and of intermolecular hydrogen bonds.

Nanoelectronic devices based on these 1D nanostructures were made to demonstrate conductivity across the anthracene units. In a typical experiment, a saturated benzene solution of **1** was dropcast on a SiO_2/Si substrate with gold microelectrodes (the distance between the adjacent metal electrodes was 3 μm). Devices featuring 1D nanostructures that cross the microelectrodes (inset of Figure 4) were used for current–voltage (*I–V*) characterization and subsequent determination of the conductivity of the 1D nanostructures at room temperature. The devices showed significant and symmetric nonlinear *I–V* responses (Figure 4) with an electric-conductance change from 8×10^{-4} to 0.011 $S\,cm^{-1}$ when the driving voltage increased from −1.5 to −3 V (Figure S3 in the Supporting Information). For the 28 devices investigated, the conductivity varied from 0.011 to 0.107 $S\,cm^{-1}$ at −3 V. In comparison with the conductivity of the reference anthracene bulk materials (ca. 10^{-10} $S\,cm^{-1}$),[24] the achieved conductivity is much higher. One possible reason for this significant increase of conductivity (three to four orders of

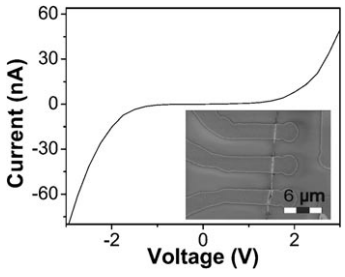

Figure 4. *I–V* curve measured over nanostructures in air and the SEM image of the device fabricated on a SiO_2/Si substrate with preprepared Au microelectrodes (inset).

magnitude enhancement) is the trace amount of solvent doping (e.g., benzene) in the nanofibres when the saturated benzene solution of **1** was dropcast on silicon substrates to form nanofibres; this has also been suggested by others.[25,26] Another possible reason could be ascribed to the smaller size of nanofibres compared with the bulk materials. For instance, the conductivity of self-assembled polyaniline nanostructures was increased with about two orders of magnitude when the diameter for the nanostructures decreased from 200 to 20 nm.[27,28] In total, it had six to seven orders of magnitude enhancement of the conductivity compared with that of anthracene bulk materials. These data suggest that the charges were transferred through the formed 1D nanostructures, through the π–π coupling of the semiconductive anthracenes. The conductivity of the nanodevices based on the self-assembled systems directly proves that the strong and extended π–π electronic communication of anthracenes is along the longitudinal axis of the 1D nanostructures. In a system based on oligopeptide-flanked pentathiophenes Tovar et al.[8] concluded, on the basis of spectroscopic evidence, that there were electronic interactions in the fibres. Here we provide a direct conductivity measurement on a device to demonstrate the conductive properties of 1D nanostructures based on π-conjugated peptides.

In summary, we have designed and synthesized a new molecule with an oligopeptide and a π-conjugated segment to generate 1D fibrous nanostructures, which can be used as components to fabricate supramolecular nanoelectronic devices. The 1D nanostructures are formed with the aid of cooperative π–π stacking of the anthracenes and intermolecular hydrogen bonding in the peptide β sheets. In addition, the strong and extended π–π electronic communication of the anthrancenes along the longitudinal axis of the 1D nanostructure allows significant conductivity along the fibre. We anticipate that research on 1D nanostructures based on biological scaffolds may promote the area of supramolecular electronics with programmed assembly and functionalization. The combination of biological scaffolds and functional molecules bridging biology with electronic properties opens the door to biosensors and the creation of hybrid electronic devices.

Experimental Section

Synthesis of 1: Compound **1** was synthesized by using standard solid-phase 9-fluorenylmethoxycarbonyl (Fmoc) chemistry on a Wang resin preloaded with Fmoc-Lys(Boc)-OH by using a Prelude peptide synthesizer from Protein Technologies. Fmoc deprotection was performed by mixing the resin in piperidine (20% v/v) in an N-methylpyrrolidone (NMP) solution for 5 min with two repetitions, followed by washing the resin with NMP (6×). For all standard amino acid couplings, Fmoc-protected amino acid (4.0 equiv relative to the resin loading), *O*-benzotriazole-*N*,*N*,*N*′,*N*′-tetramethyluronium hexafluorophosphate (HBTU, 4 equiv) in NMP, and diisopropylethylamine (DIPEA, 16 equiv) in NMP were added to the reaction vessel and mixed for 20 min in an nitrogen atmosphere. This amino-acid coupling step was repeated for another 20 min. After the LLKK amino acids had been attached to the resin, the N-terminal Fmoc was deprotected and anthracene-9-carboxylic acid (4.0 equiv), HCTU (4.0 equiv), and DIPEA (16 equiv) were added to the reaction vessel to introduce the functional unit. The resin was washed with NMP (6×) and CH_2Cl_2 (4×) and allowed to dry under high vacuum. Peptide cleavage from the resin and removal of side-chain protecting groups were accomplished by stirring the resin in a mixture of trifluoroacetic acid (TFA), water, and triisopropylsilane (Tis, 5 mL, 96:2:2% v/v) for 1 h at room temperature. The resin was removed by filtration and washed with a small amount of TFA. The peptide was precipitated out from the filtrate by the addition of cold diethyl ether (50 mL). The precipitate was centrifuged and the supernatant was poured out, leaving the crude peptide. The crude peptide was dissolved in water and lyophilized. The peptide was then dissolved in water with TFA (0.1%) and purified by preparative HPLC to yield **1**. ^{1}H NMR (D_2O, 400 MHz): $\delta = 8.70$ (s, 1H), 8.15 (d, $J = 8.4$ Hz, 2H), 7.97–7.91 (m, 2H), 7.64–7.56 (m 4H), 4.46 (t, $J = 6.4$ Hz, 1H), 4.18–4.15 (m, 1H), 2.98–2.93 (m, 2H), 2.91–2.85 (m, 2H), 1.86–1.54 (m, 17H), 1.46–1.35 (m, 5H), 1.05–1.04 (m, 3H), 1.0–0.95 ppm (m, 10H); MS (ESI$^+$, H_2O/MeCN): *m*/*z*: calcd for $C_{39}H_{57}N_6O_6^+$: 705.43 $[M+H]^+$; found: 705.8; calcd for $0.5C_{39}H_{58}N_6O_6^{2+}$: 353.22 $[0.5M+H]^+$; found: 353.5; calcd for $C_{78}H_{113}N_{12}O_{12}^+$: 1409.86 $[2M+H]^+$; found: 1409.8.

Device fabrication and measurements: Two-end devices were fabricated as follows: Au electrodes were fabricated on a Si/SiO_2 substrate by a standard photolithography method. A solution of **1** was dropcast on the substrate, and the formed fibrils crossing the microelectrodes were chosen for the conductivity measurement. All electrical measurements were performed in ambient conditions with a Keithley semiconductor parameter analyzer (model 4200-SCS).

Acknowledgements

X.C. acknowledges support from the National Research Foundation of Singapore (NRF-RF2009–04) and SUG of Nanyang Technological University.

Keywords: electronics · nanotechnology · self-assembly · supramolecular chemistry · π-conjugated peptides

[1] A. P. H. J. Schenning, E. W. Meijer, *Chem. Commun.* **2005**, 3245–3258.
[2] R. J. Li, W. P. Hu, Y. Q. Liu, D. B. Zhu, *Acc. Chem. Res.* **2010**, *43*, 529–540.
[3] S. Y. Park, A. K. Lytton-Jean, B. Lee, S. Weigand, G. C. Schatz, C. A. Mirkin, *Nature* **2008**, *451*, 553–556.
[4] S. G. Zhang, *Nat. Biotechnol.* **2003**, *21*, 1171–1178.
[5] H. G. Cui, M. J. Webber, S. I. Stupp, *Biopolymers* **2010**, *94*, 1–18.
[6] J. D. Hartgerink, E. Beniash, S. I. Stupp, *Science* **2001**, *294*, 1684–1688.
[7] Y. Yanlian, K. Ulung, W. Yiumei, A. Horii, H. Yokoi, Z. Shuguang, *Nano Today* **2009**, *4*, 193–210.
[8] S. R. Diegelmann, J. M. Gorham, J. D. Tovar, *J. Am. Chem. Soc.* **2008**, *130*, 13840–13841.
[9] D. A. Stone, L. Hsu, S. I. Stupp, *Soft Matter* **2009**, *5*, 1990–1993.
[10] H. Shao, T. Nguyen, N. C. Romano, D. A. Modarelli, J. R. Parquette, *J. Am. Chem. Soc.* **2009**, *131*, 16374–16376.
[11] M. O. Guler, R. C. Claussen, S. I. Stupp, *J. Mater. Chem.* **2005**, *15*, 4507–4512.
[12] J. D. Tovar, R. C. Claussen, S. I. Stupp, *J. Am. Chem. Soc.* **2005**, *127*, 7337–7345.
[13] J. D. Tovar, B. M. Rabatic, S. I. Stupp, *Small* **2007**, *3*, 2024–2028.
[14] H. X. Xu, A. K. Das, M. Horie, M. S. Shaik, A. M. Smith, Y. Luo, X. F. Lu, R. Collins, S. Y. Liem, A. Song, P. L. A. Popelier, M. L. Turner, P. Xiao, I. A. Kinloch, R. V. Ulijn, *Nanoscale* **2010**, *2*, 960–966.

[15] H. Cui, T. Muraoka, A. G. Cheetham, S. I. Stupp, *Nano Lett.* **2009**, *9*, 945–951.
[16] S. Ando, J.-i. Nishida, E. Fujiwara, H. Tada, Y. Inoue, S. Tokito, Y. Yamashita, *Chem. Mater.* **2005**, *17*, 1261–1264.
[17] H. Meng, F. P. Sun, M. B. Goldfinger, G. D. Jaycox, Z. G. Li, W. J. Marshall, G. S. Blackman, *J. Am. Chem. Soc.* **2005**, *127*, 2406–2407.
[18] L. Jiang, Y. Y. Fu, H. X. Li, W. P. Hu, *J. Am. Chem. Soc.* **2008**, *130*, 3937–3941.
[19] Y. K. Che, X. M. Yang, G. L. Liu, C. Yu, H. W. Ji, J. M. Zuo, J. C. Zhao, L. Zang, *J. Am. Chem. Soc.* **2010**, *132*, 5743–5750.
[20] L. Giribabu, A. A. Kumar, V. Neeraja, B. G. Maiya, *Angew. Chem.* **2001**, *113*, 3733–3736; *Angew. Chem. Int. Ed.* **2001**, *40*, 3621–3624.
[21] Z. C. Zuo, H. B. Liu, X. D. Yin, H. Y. Zheng, Y. L. Li, *J. Coll. Inter. Sci.* **2009**, *329*, 390–394.
[22] J. M. W. Chan, J. R. Tischler, S. E. Kooi, V. Bulovic, T. M. Swager, *J. Am. Chem. Soc.* **2009**, *131*, 5659–5666.
[23] T. Katoh, Y. Inagaki, R. Okazaki, *Bull. Chem. Soc. Jpn.* **1997**, *70*, 2279–2286.
[24] D. D. Eley, A. S. Fawcett, M. R. Willis, *Nature* **1963**, *200*, 255–255.
[25] Y. K. Che, A. Datar, K. Balakrishnan, L. Zang, *J. Am. Chem. Soc.* **2007**, *129*, 7234–7235.
[26] M. H. Huang, U. Schilde, M. Kumke, M. Antonietti, H. Coelfen, *J. Am. Chem. Soc.* **2010**, *132*, 3700–3707.
[27] Z. Zhang, L. Wang, J. Deng, M. Wan, *React. Funct. Polym.* **2008**, *68*, 1081–1087.
[28] M. Delvaux, J. Duchet, P.-Y. Stavaux, R. Legras, S. Demoustier-Champagne, *Synth. Met.* **2000**, *113*, 275–280.

Received: December 31, 2010
Published online: March 14, 2011

